September 2006

Novel mesoscale defect structure on NiO(1 0 0) surfaces by atomic force microscopy

S. C. Petitto
University of Nebraska - Lincoln

Cindy L. Berrie
University of Kansas, cberrie@ku.edu

Marjorie Langell
University of Nebraska - Lincoln, mlangell1@unl.edu

Published in *Surface Science* 600:17 (September 1, 2006), pp. L229–L235. doi:10.1016/j.susc.2006.06.005 http://www.sciencedirect.com/science/journal/00396028

Submitted March 11, 2006; revised June 6, 2006; published online June 30, 2006.

Surface Science Letters

Novel mesoscale defect structure on NiO(1 0 0) surfaces by atomic force microscopy

S.C. Petitto[a], C.L. Berrie[b], and M.A. Langell[a,*]

[a]*Department of Chemistry, University of Nebraska–Lincoln, Lincoln, NE 68588-0304, United States*
[b]*Department of Chemistry, University of Kansas, Lawrence, KS 66045-7582, United States*
* Corresponding author. Email: mlangell@unlserve.unl.edu (M.A. Langell).

Abstract: Cleaved NiO(1 0 0) surfaces were imaged with atomic force microscopy (AFM) to determine defect concentrations and morphology. Random (0 1 0) and (0 0 1) oriented steps, which have been previously characterized, were the most common defect observed on the cleaved surface and formed with step heights in multiples of 2.1 Å, the Ni–O nearest-neighbor distance, and terrace widths in the range of 25–100 nm. In addition, the surface showed novel mesoscale (~0.5–2 μm) square pyramidal defects with the pyramid base oriented along (1 0 0) symmetry related directions. Upon etching, the pyramidal defects converted to more stable cubic pits, consistent with (1 0 0) symmetry related walls. The square pyramidal pits tended to cluster or to form along step edges, where the weakened structure is more susceptible to surface deformations. Also, a small concentration of square pyramidal pits, oriented with the base of the pyramid along (0 1 1), was observed on the cleaved NiO surfaces. For comparison purposes, chemical mechanical polished (CMP) NiO(1 0 0) substrates were imaged with AFM. Defect concentrations were of comparable levels to the cleaved surface, but showed a different distribution of defect types. Long-ranged stepped defects were much less common on CMP substrates, and the predominant defects observed were cubic pits with sidewalls steeper than could be accurately measured by the AFM tip. These defects were similar in size and structure to those observed on cleaved NiO(1 0 0) surfaces that had been acid etched, although pit clustering was more pronounced for the CMP surfaces.

Keywords: Nickel oxide, Scanning probe techniques, Surface structure, Surface morphology, Topography

Transition metal oxides (TMO) are relevant to a wide range of heterogeneous applications, both as bulk materials and as overlayers that form on ambient-exposed transition metal substrates. The surface properties of these materials, in turn, are often highly influenced by surface defect structure [1], [2], [3] and [4]. Defects have been shown to be important in TMO electronic, magnetic, and chemical properties and span a wide range of scale, including oxygen vacancies [1], [2], [3], [5], [6], [7] and [8], metal interstitials and adatoms [1] and [9], crystal shear planes [4] and [10], step-defects [4], [10], [11] and [12], meso- to macroscopic scale pits, protrusions, and related large-scale imperfections [13], [14] and [15], the latter of which often have a complicated morphology with a range of atomic-scale defects in their own right [16], [17], [18] and [19]. The surface defect nature may be influenced by bulk structure and impurity concentration [1], [4] and [20], introduced by surface preparation methods [12] and [21], or result from chemical reactivity and corrosion properties of the substrate surface [1], [2], [3], [5], [6] and [22].

For single crystal TMOs, surface integrity is dependent upon sample preparation, and protocols developed for these materials generally include either crystal cleavage or chemical mechanical polishing (CMP). NiO(1 0 0) is a prototypical rocksalt oxide that can be produced by either method in high quality, since its (1 0 0) orientation represents a very stable cleavage plane due to the closest-packed, nonpolar nature of

the surface and since it also responds favorably to annealing treatments following CMP without change in chemical composition due to the very stable nature of octahedral Ni^{2+} in the solid state. Among its numerous materials applications, nickel oxide is an active component in mixed-metal oxide partial oxidation catalysis [23], [24], [25] and [26], in chemical sensor technology [27], [28], [29], [30] and [31], and as a cathode base material in solid oxide fuel cells [32], [33], [34] and [35], and high temperature power generation [36] and [37]. Its bulk antiferromagnetic nature lends itself to use in coupled layer magnetic storage media [38], [39] and [40] and the magnetic behavior of NiO nanoparticles is suitable for spin valves important in the rapidly developing field of spintronics [41], [42], [43] and [44]. NiO surface properties have been well investigated [19], [45], [46], [47], [48], [49], [50], [51], [52], [53] and [54] and the band structure [55], [56], [57], [58], [59], [60] and [61] and crystallography of the ideal surface [62] and [63] are well-known. The NiO(1 0 0) cleavage plane [45], [62], [63] and [64] can produce, to within reasonable tolerances, well-ordered, stoichiometric substrates although cleaved surfaces have been reported to contain randomly-spaced step defects, approximately 25–100 nm apart, with the step heights in multiples of 2.1 Å, the Ni–O nearest-neighbor distance [52] and [54]. These features have not, however, been extensively characterized.

We present here atomic force microscopy (AFM) data that indicate even high quality NiO(1 0 0) surfaces contain small numbers of micrometer to sub-micrometer scale cubic and square pyramidal pit defects, in addition to long range, randomly-spaced step defects which we show are clearly related to the underlying (1 0 0) substrate symmetry and are influential in subsequent pit defect formation and structure. The most prevalent morphology of the square pyramidal defect forms with its base parallel to (0 0 1) and (0 1 0) and nominally consistent with four symmetrically equivalent sets of (0 1 1) surface walls. A less prevalent orientation, with the base rotated 45° from (0 0 1) and (0 1 0) with (1 1 1) walls, is also seen at about 15% of the total pit defect concentration. While pit defects persist after chemical mechanically polishing, their predominant morphology is cubic in form, with (0 0 1) and (0 1 0) walls and flat (1 0 0) bottoms. Similar cubic pit defect structure is observed after acid etching of cleaved NiO(1 0 0) substrates. The results indicate that mesoscale step and pit defects are prevalent on this rocksalt TMO substrate and that the three dimensional nature of their structure is surprisingly well-ordered and easily related to bulk symmetry considerations.

The NiO samples were cleaved from a single crystal boule (First Reaction, Hampton Falls, NH) in air immediately prior to atomic force microscopy (AFM) to produce substrates with the surface normal oriented along the (0 0 1) direction. For comparison, cut and polished NiO(1 0 0) surfaces also were studied. The polished samples, approximately 10 mm × 10 mm × 2 mm, were taken from the same boule, oriented with back Laue diffraction to within 0.25° of (0 0 1), and chemically mechanically polished (CMP) to a high luster using standard polishing methods [65] and [66]. Representative samples were then analyzed for surface order and stoichiometry using complementary surface sensitive techniques in ultrahigh vacuum (UHV) [67].

AFM images of the NiO(1 0 0) substrates were obtained with one of two Digital Instruments (VEECO) Nanoscope E systems. The AFM images were acquired in air in contact mode using a silicon nitride (Si_3N_4) tip (spring constant $k = 0.12$ N/m, VEECO) with 512 × 512 line resolution. Scan size was varied from survey scans at 50–100 μm to higher resolution scans of features of interest ~1 μm in dimension. The only processing performed on the images reported here was flattening.

The freshly cleaved (1 0 0) surface shows varying step height defects (Fig. 1) with random terrace widths ranging primarily from 25 to 100 nm in spacing, along with sparsely distributed pyramidal, "star" shaped pits at approximately 1.0×10^{-2} defects/μm^2. The steps run along either (1 0 0) or (0 1 0) directions, and while some steps seem eventually to deviate from these stable lattice directions, the "curved" segments are actually composed of a series of sequential (0 0 1) and (0 1 0) steps and kinks to give rise to the long-ranged, curved appearance. Step densities, step heights and terrace widths are in agreement with those previously reported for air-cleaved NiO(1 0 0) [54].

The star-shaped surface features are shown in greater detail in Fig. 2 to be pits with nominally square pyramidal shape consistent with (1 1 0) symmetry-related walls, and have not previously been reported for air-cleaved rocksalt monoxide samples [54]. Pit widths ranging from 400 to 2500 nm and depths from 40 to 570 nm were observed on the freshly cleaved NiO(1 0 0) surfaces. The square pyramidal pits were not randomly distributed throughout the surface, but tended to form in clusters and along step edges. A convolution of the defect shape with the cone angle and shape of the probe tip makes it difficult to determine the angle between the faces precisely [68]. However, the angle of opposite faces in the square pyramidal defect (Fig. 2c) is consistent with the 90° angle expected between the symmetry related (1 1 0) planes after convolution with the AFM tip shape. Cross-sectional profiles shown below also support this model of the defect structure. It should be noted that the (1 1 0) faces of these "pyramidal" defects are not perfectly formed, in part because there are step defects along the faces that distort the pyramid walls.

In addition to the defect shape, the AFM images also provide information about the orientation of the defects. As shown in Fig. 1, the (0 0 1) and (0 1 0) oriented steps are easily identifiable in AFM and provide a reliable reference for determining the orientation of features that have formed on NiO(1 0 0). Step edge referencing also avoids inaccuracies resulting from tip size and shape effects, which limit the accuracy of the wall angle measurements above. Fig. 1c and d show the pyramid base oriented along the (0 0 1) and (0 1 0) rocksalt lattice directions and parallel to the steps of the cleaved NiO(1 0 0) sample. The lowest Miller index surface (Fig. 3) that fits this requirement is the (1 1 0) crystal face, a moderately close packed, charge-neutral surface, although not as efficient in balancing cation/anion Cou-

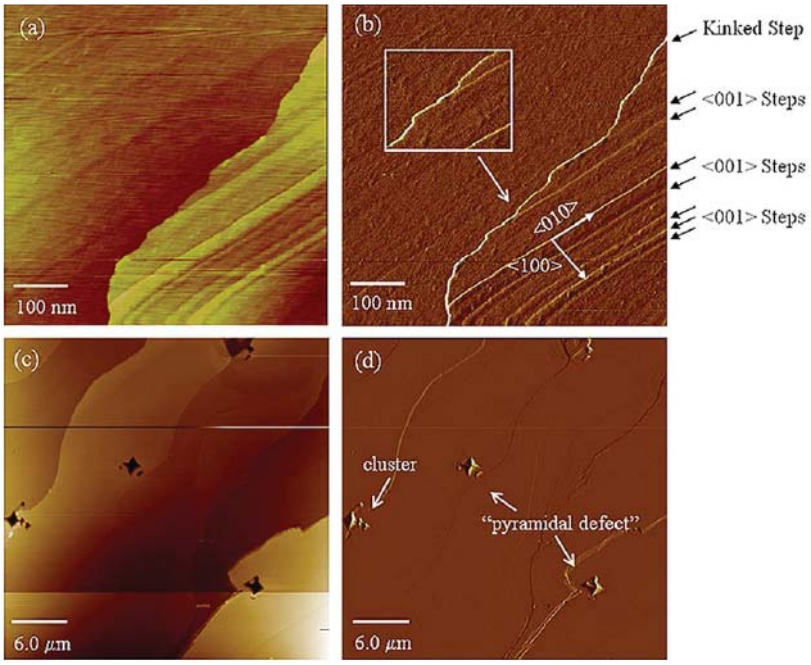

Figure 1. AFM images of freshly cleaved NiO(1 0 0) surfaces in air with steps running along the (1 0 0) and (0 1 0) directions (a) in height mode and (b) deflection mode, with the inset showing a detailed expansion of steps and kinks, and a wider range scan in (c) height mode and (d) deflection mode showing scattered pyramidal defects.

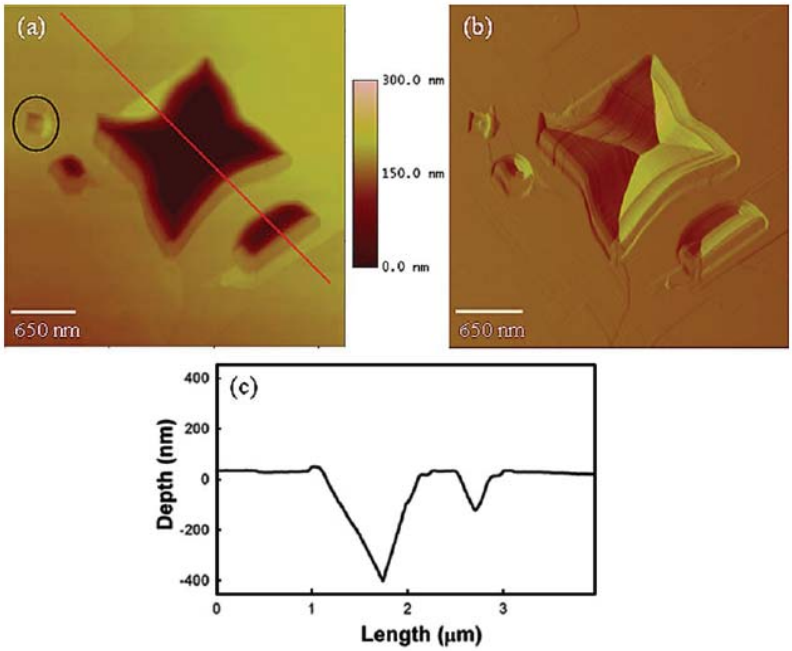

Figure 2. AFM of a freshly cleaved NiO(1 0 0) surface in (a) height mode and (b) in deflection mode showing several star-shaped pyramidal pits and a trough (lower right hand corner) in which the pit defect has only formed (1 1 0) walls along one crystallographic direction. The circled feature in (a) is a 45° rotated pyramid. In (c), a cross-sectional profile is taken through the large square pyramid along the scan line shown in red in (a).

lombic forces as the (1 0 0) cleavage plane. However, metastable surface orientations are often observed when activation barriers to form lower energy planes are prohibitive, for example in vicinally-stepped substrates produced by cutting at a small angle relative to a stable surface plane [67], [69], [70] and [71] and in epitaxial thin films templated by an underlying, stable substrate [72], [73], [74] and [75]. The random, naturally occurring steps observed here for NiO(1 0 0) are another example of metastable

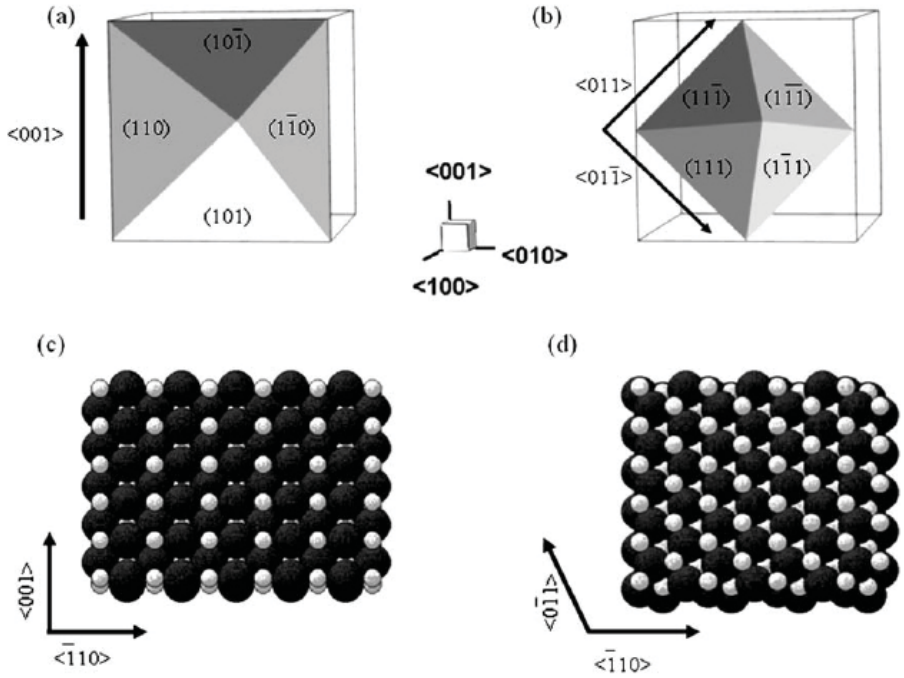

Figure 3. Models of the square pyramid defect structure of NiO(1 0 0) for square pyramidal pits in which (a) bases are oriented along (0 0 1) with (1 1 0) surface planes and (b) bases are oriented along the (0 1 1) with (1 1 1) surface planes. The rocksalt surface termination structures for the (c) (1 1 0) and (d) (1 1 1) faces also are shown.

features. Diffusion from step-edge to step-edge could, in principle, create a flat, step-defect free substrate, but diffusion rates are insufficient at room temperature to mobilize the surface atoms to flatten the stepped surface, and the steps are stable over the course of the AFM imaging experiment.

A small number (<15%) of the square pyramidal pit defects were observed on the cleaved NiO(1 0 0) substrate with the pyramidal base rotated by 45° from the (0 1 0) and (0 1 0) directions (Fig. 2). The circled feature in Fig. 2a shows a shallow square pyramidal pit defect, about 30 nm deep, in which the square pyramidal base is rotated by 45° in relation to the main defect orientation of the larger, (1 1 0)-walled, pit to its right. A square pyramid oriented in this manner should have (1 1 1) sidewalls (Fig. 3b) if it is to produce a close packed surface plane consistent with base orientation of (0 1 1) and < 0 1 $\bar{1}$ >. Although the (1 1 1) rocksalt plane fits these requirements, it produces a polar surface with alternating hexagonal layers of cations and anions (Fig. 3d). NiO(1 1 1) might, therefore, not be expected to be particularly stable for surface termination, and thus in surface defect formation. However, NiO(1 1 1) surfaces have been reported in metastable form in the literature [72], [76] and [77] although their formation has been generally accompanied by some sort of surface stabilization such as hydroxylation [72] and [76] or reconstruction of the outermost layer [77] to stabilize the strong Coulombic repulsion expected from simple bulk termination.

Etching the cleaved NiO(1 0 0) surface in H_2SO_4 introduces new morphology in defect structure. After 10 min in 40 °C H_2SO_4 (Fig. 4), cubic pits with well-formed "flat bottoms" are observed. This is expected if the (1 1 0) walls are etched away resulting in the formation of the more stable (1 0 0) plane at the base of the defect. The circled feature in Fig. 4a shows an example of well-formed cubic defects and the cross-sectional profile (Fig. 4c and d) clearly indicates cubic shape. Square pyramidal pits are still observed but show evidence of etching and the formation of flat, (1 0 0) bottom faces as well. Particularly interesting is the defect that has formed along a step edge (boxed feature in Fig. 4a). The steps on the NiO surface are clearly apparent and track the observed step structure outside the defect as shown in the three cross-sectional profiles (Fig. 4e and f) at different positions along the length of the defect. The scan perpendicular to the step along the line that includes the square pyramid's apex also shows the step structure to be superimposed upon the square pyramid defect wall, although the steeper slope of the defect wall at the apex makes the step structure harder to resolve given the finite dimensions of the AFM tip.

For comparison to the defect structure of the cleaved surface, chemical mechanical polished NiO(1 0 0) substrates also were studied. The samples were previously characterized in UHV [67], but had been stored in ambient laboratory air for a period of several days to several weeks. The CMP surfaces gave comparable AFM results, regardless of length of time exposed to the ambient. Unlike the cleaved NiO(1 0 0) substrate, step defects are not easily identified on CMP surfaces, and clusters of cubic defects, consistent with (0 0 1) sidewalls are observed with an average depth of 300 nm (100 nm standard deviation) and an average width of 1000 nm (300 nm standard deviation). The average pit depth and width are sim-

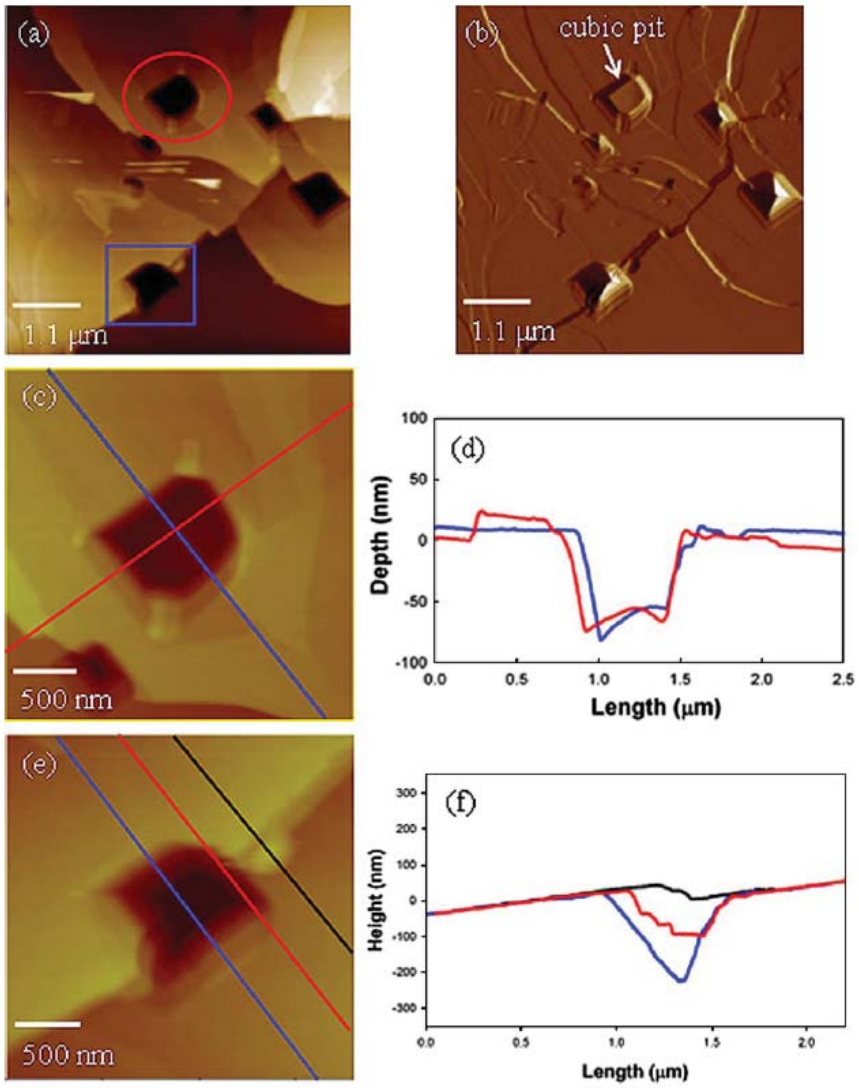

Figure 4. AFM of cleaved NiO(1 0 0) after 10 min in 40 °C H_2SO_4 in (a) height mode and (b) deflection mode for a cluster of pits. The red circle indicates a well-formed cubic pit, enlarged in (c) the height mode and (d) the corresponding cross-sectional line profiles along the two symmetry related (1 0 0) and (0 1 0) directions. Preservation of the step structure within the pit from the blue square in (a) is shown in an enlarged (e) height image with the cross-sectional profiles (f) through the apex and side of the pit.

ilar to the larger (0 1 1)-walled defects found on the cleaved surface. The (0 0 1)-walled defects on the CMP NiO(1 0 0) surface tend to cluster, as shown in Fig. 5a and c, and the line scan analysis of an individual pit (Fig. 5e and g) indicates that the walls and the bottom are square and flat, aside from the distortion expected from the convolution with the shape of the probe tip.

In the CMP process, abrasive particles can embed themselves into the surface and spin deep into the substrate resulting in non-uniform pits of varying widths and depths [66]. Pits tend to form in weakened areas of the surface [65] and [66] and once the initial surface pit is formed, the surface surrounding the pit is further weakened, making it easier for other pits to form. This results in the clustering of pits shown in Fig. 5a, which clearly depicts regions of high and low pit density. Liquids are used in the CMP process to suspend the polishing abrasive and to act as a lubricant; however, they also can result in substrate etching. In the present studies, the CMP slurry composed of Al_2O_3, ultrapure spectrophotometric grade white glycerin, and distilled water has etched the surface resulting in cubic, (1 0 0)-walled, flat-bottomed defects similar in morphology to the acid-etched NiO(1 0 0) cleaved substrates.

NiO(1 0 0) surfaces have been imaged with AFM and present novel, symmetric square pyramidal and cubic defect structures not previously reported for rocksalt oxide substrates. The cleaved surfaces were dominated by random step defects that formed along stable (0 0 1) and (0 1 0) directions, but also showed square pyramidal pits with (0 1 1) walls. Etching the NiO(1 0 0) surfaces, either by acid treatment of cleaved substrates or undesired side reactions during chemical mechanical polishing, resulted in (0 1 0) and (1 1 0)-walled cubic pits

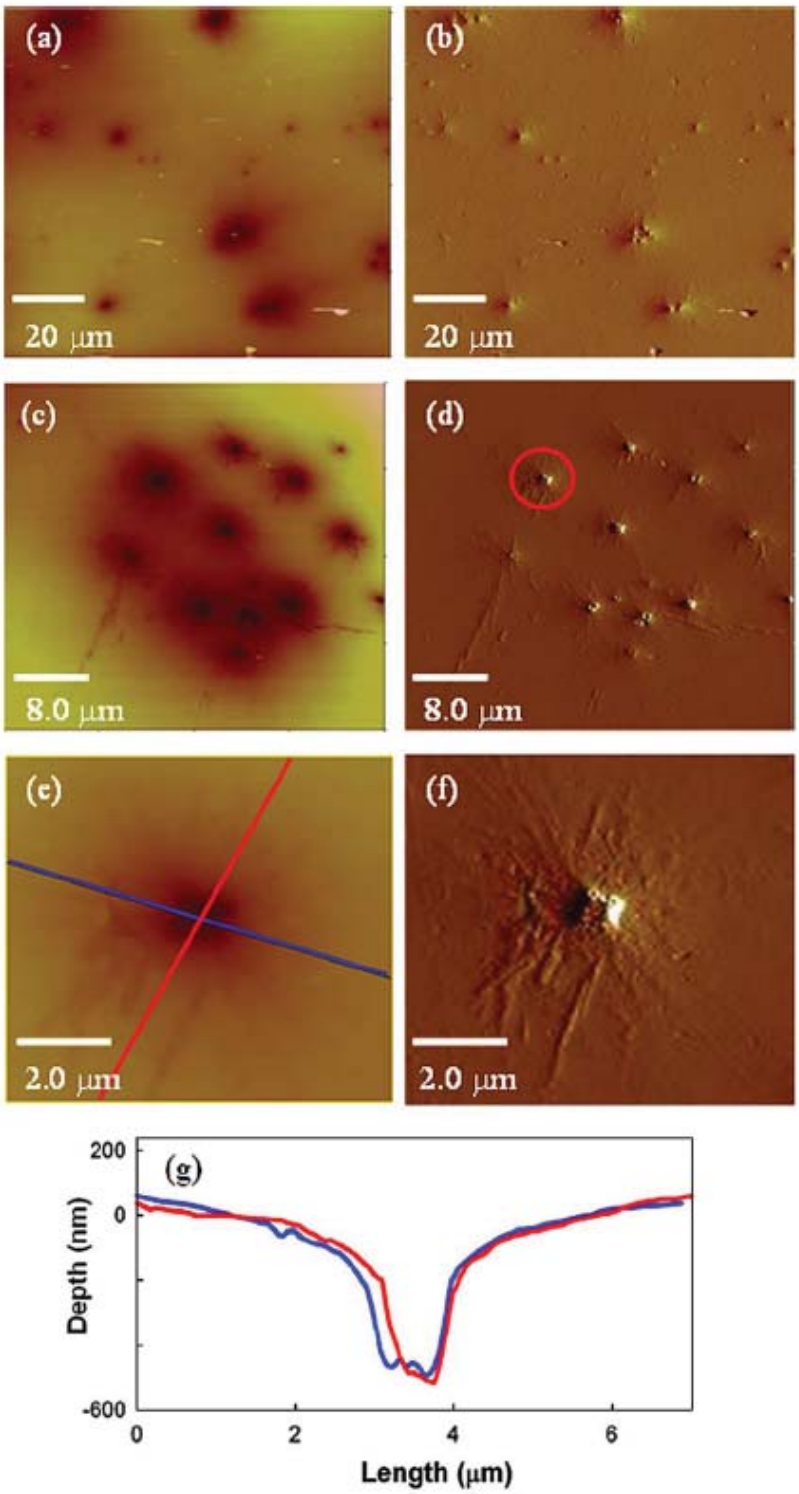

Figure 5. AFM of CMP prepared NiO(1 0 0) surface in (a) height mode and (b) deflection mode for an 100 μm image that shows areas of low and high pit density, (c) height mode and (d) deflection mode a cluster of pits covering ~40 μm region, and (e) the height mode and (f) deflection mode image of the individual pit circled in red in (d) with the corresponding (g) cross-sectional line profiles, indicating the walls and the bottom of these pits are square and flat. Each defect on this scale, when expanded, shows a cluster structure similar to that of (a).

with nominally flat (1 0 0) bottoms and very low numbers of random step defects. Surface defects tended form in weaken areas of the surface, which resulted in clustering of pits defect among each other and along step defects.

Acknowledgements

We gratefully acknowledge support from NSF Grant CHE-0213320 and the University of Nebraska Big 12 Faculty Fellowship program. The authors also would like to thank E. Papastavros for her help in acquiring the AFM images.

References

[1] V.E. Henrich, *Chem. Phys. Solid Surf.* **9** (2001), p. 1.
[2] D.A. Bonnell, *Prog. Surf. Sci.* **57** (1998), p. 187.
[3] U. Diebold, *Surf. Sci. Rep.* **48** (2003), p. 52.
[4] J. Wollschlaeger, *Defect Diffus. Forum* **164** (1998), p. 37.
[5] W. Weiss and R. Wolfgang, *Prog. Surf. Sci.* **70** (2002), p. 1.
[6] H.J. Freund, *Faraday Discuss.* **114** (1999), p. 1.
[7] N. Lopez and S. Valeri, *Phys. Rev. B* **70** (2004), p. 125428/1.
[8] G. Pacchioni, *Chem. Phys. Chem.* **4** (2003), p. 1041.
[9] E. Dokou, W.E. Farneth and M.A. Barteau, *Stud. Surf. Sci. Catal.* **130D** (2000), p. 3167.
[10] R.A. Bennett, P. Stone and M. Bowker, *Faraday Discuss.* **114** (1999), p. 267.
[11] M. Baeumer, D. Cappus, H. Kuhlenbeck, H.J. Freund, G. Wilhelmi, A. Brodde and H. Neddermeyer, *Surf. Sci.* **253** (1991), p. 116.
[12] F.H. Jones, K. Rawlings, R.A. Dixon, T.W. Fishlock and R.G. Egdell, *Surf. Sci.* **460** (2000), p. 277.
[13] N. Casillas, S.J. Charlebois and W.H. Smyrl, *J. Electrochem. Soc.* **140** (1993), p. L142.
[14] L.E. Matson, H. Erhart, M. Lee and R.A. Rapp, *Metallug. Trans. A* **15** (1984), p. 2241.
[15] A. Gebert, F. Schneider and K. Mummert, *Nucl. Eng. Des.* **174** (1997), p. 327.
[16] L. Long and J.C. Yang, *Mater. High Temp.* **20** (2003), p. 601.
[17] G. Waston, *Radiat. Eff. Defects Sol.* **157** (2002), p. 773.
[18] C.M. Foster, G.R. Bai, R. Csencsits, J. Vetrone, R. Jammy, L.A. Willis, E. Carr and J. Amano, *J. Appl. Phys.* **81** (1997), p. 2349.
[19] J.A. Eastman, F. Schmuckle, M.D. Vaudin and S.L. Sass, *Adv. Ceram.* **10** (1984), p. 324.
[20] W. Przybilla and M. Schuetze, *Oxid. Met.* **58** (2002), p. 103.
[21] V. Maurice, S. Cadot and P. Marcus, *Surf. Sci.* **471** (2001), p. 43.
[22] J.Y. Ranke and W. Weiss, *J. Phys. Chem. B* **104** (2000), p. 3224.
[23] Y.H. Hu and E. Ruckenstein, *Catal. Rev.* **44** (2002), p. 423.
[24] M. Nurunnabi, S. Kado, K. Suzuki, K. Fujimoto, K. Kunimori and K. Tomishige, *Catal. Commun.* **7** (2006), p. 488.
[25] A. Zecchina, D. Scarano, S. Bordiga, G. Spoto and C. Lamberti, *Adv. Catal.* **46** (2001), p. 265.
[26] Y. Wu, Y. He, T. Chen, W. Weng and H. Wan, *Appl. Surf. Sci.* **252** (2006), p. 5220.
[27] C. Cantalini, M. Post, D. Buso, M. Guglielmi and A. Martucci, *Sens. Actuat. B: Chem.* **B108** (2005), p. 184.
[28] K. Arshak and O. Korostynska, *Sens. Actuat. A: Phys.* **A113** (2004), p. 319.
[29] A. Vollmer, J.D. Lipp, J.R.I. Lee, G.E. Derbyshire and T. Rayment, *Anal. Chem.* **75** (2003), p. 6571.
[30] M. Shiotsuka, S. Takase and Y. Shimizu, *Chem. Sens.* **17** (2001), p. 381.
[31] P. Umadevi and C.L. Nagendra, *Sens. Actuat. A: Phys.* **A96** (2002), p. 114.
[32] M. Yoshikawa, Y. Mugikura, T. Watanabe, T. Nishimura, T. Yagi and Y. Fujita, *Electrochem.* **70** (2002), p. 183.
[33] J. Han, S.-G. Kim, S.P. Yoon, S.W. Nam, T.-H. Lim, I.-H. Oh, S.-A. Hong and H.C. Lim, *J. Power Sources* **106** (2002), p. 153.
[34] A. Wijayasinghe, C. Lagergren and B. Bergman, *Fuel Cells* **2** (2003), p. 181.
[35] D.J. Moon and J.W. Ryu, *Catal. Lett.* **89** (2003), p. 207.
[36] K.R. Prasad and N. Miura, *Appl. Phys. Lett.* **85** (2004), p. 4199.
[37] P.A. Nelson, J.M. Elliott, G.S. Attard and J.R. Owen, *J. New Mater. Electrochem. Syst.* **5** (2002), p. 63.
[38] R. Gomez-Abal, O. Ney, K. Satitkovitchai and W. Hubner, *Phys. Rev. Lett.* **92** (2004), p. 227402/1.
[39] J.-W. Park, J.-W. Park, D.-Y. Kim and J.-K. Lee, *J. Vac. Sci. Technol. A* **23** (2005), p. 1309.
[40] G. Lefkidis, O. Ney, Y. Pavlyukh, K. Satitkovitchai and W. Huebner, *NATO Sci. Ser. II. Math. Phys. Chem.* **164** (2004), p. 19.
[41] M. Pinarbasi, S. Metin, H. Gill, M. Parker, B. Gurney, M. Carey and C. Tsang, *J. Appl. Phys.* **87** (2000), p. 571.
[42] S. Li, T.S. Plaskett, P.P. Freitas, J. Bernardo, B. Almeida and J.B. Sousa, *IEEE Trans. Magn.* **34** (1998), p. 3772.
[43] R.H. Taylor, R. O'Barr, S.Y. Yamamoto and B. Dieny, *J. Appl. Phys.* **85** (1999), p. 5036.
[44] M. Pinarbasi, S. Metin, H. Gill, M. Parker, B. Gurney, M. Carey and C. Tsang, *J. Appl. Phys.* **87** (2000), p. 5714.
[45] P.W. Tasker, *J. Phys. C: Solid State Phys.* **12** (1979), p. 4977.
[46] C.G. Kinniburgh and J.A. Walker, *Surf. Sci.* **63** (1977), p. 274.
[47] F.P. Netzer and M. Prutton, *J. Phys. C* **8** (1975), p. 2401.
[48] A. Freitag, V. Staemmler, D. Cappus, C.A. Ventrice Jr., K. Al Shamery, H. Kuhlenbec and H.-J. Freund, *Chem. Phys. Lett.* **210** (1993), p. 10.
[49] N.S. McIntyre and M.G. Cook, *Anal. Chem.* **47** (1975), p. 2208.
[50] K.W. Wulser and M.A. Langell, *Surf. Sci.* **314** (1994), p. 385.
[51] K.W. Wulser, B.H. Hearty and M.A. Langell, *Phys. Rev. B* **46** (1992), p. 9724.
[52] S. Imaduddin and R.J. Lad, *Surf. Sci.* **290** (1993), p. 35.
[53] M.R. Castell, S.L. Dudarev, C. Muggelberg, A.P. Sutton, G.A.D. Briggs and D.T. Goddard, *J. Vac. Sci. Technol. A* **16** (1998), p. 1055.
[54] H. Hosoi, K. Sueoka, K. Hayakawa and K. Mukasa, *Appl. Surf. Sci.* **157** (2000), p. 218.
[55] Z.-X. Shen, J.W. Allen, P.A.P. Lindberg, D.S. Dessau, B.O. Wells, A. Borg, W. Ellis, J.S. Kang, S.-J. Oh, I. Lindau and W.E. Spicer, *Phys. Rev. B* **42** (1990), p. 1817.
[56] J. Zaanen, G.A. Sawatzky and J.W. Allen, *Phys. Rev. Lett.* **55** (1985), p. 418.
[57] T. Oguchi, K. Terakura and A.R. Williams, *Phys. Rev. B* **28** (1983), p. 6443.
[58] V.I. Anisimov, J. Zaanen and O.K. Anderson, *Phys. Rev. B* **44** (1991), p. 943.
[59] N.M. Harrison, *Comput. Phys. Commun.* **137** (2001), p. 59.
[60] J. Bala, M. Andrzej and J. Zaanen, *Phys. Rev. B* **61** (2000), p. 13573.
[61] M. Arai and T. Fujiwara, *Phys. Rev. B* **51** (1995), p. 1477.
[62] W. Nuebeck, C. Vettier, F. de Bergevin, F. Yakhou, D. Mannix, O. Bengone, M. Alouani and A. Barbier, *Phys. Rev. B* **63** (2001), p. 134430/1.
[63] V.E. Henrich, *Rep. Prog. Phys.* **48** (1985), p. 1481.
[64] P.A. Cox, Transition Metal Oxides: An Introduction to Their Electronic Structure and Properties, Oxford University Press, Oxford (1992).
[65] E.A. Colbourn, W.C. Mackrodt and P.W. Tasker, *Physics* **129** (1985), p. 397.
[66] L.E. Samuels, South Bay Technology Technical Paper # 269, South Bay Technology, CA, 1985.
[67] L.E. Samuels, Metallographic Polishing by Mechanical Methods, Pitman Press, London (1971).
[68] S.C. Petitto, E.M. Marsh and M.A. Langell, *J. Phys. Chem. B* **110** (2006), p. 1309.
[69] Digital Instruments, Multimode Atomic Force Microscope Manual, Veeco Instruments Inc., Woodbury, New York (2001) Chapter 4.
[70] W.P. Ellis and R.L. Schwoebel, *Surf. Sci.* **11** (1968), p. 82.
[71] H. Onishi, T. Aruga, C. Egawa and Y. Iwasawa, *Surf. Sci.* **193** (1988), p. 33.
[72] P.W. Murray, F.M. Leibsle, H.J. Fisher, C.F.J. Flipse and G. Thornton, *Surf. Sci.* **321** (1994), p. 217.
[73] P.W. Murray, F.M. Leibsle, C.A. Muryn, H.J. Fisher and C.F.J. Thornton, *Phys. Rev. Lett.* **72** (1994), p. 689.
[74] M.A. Langell and M.H. Nassir, *J. Phys. Chem.* **99** (1995), p. 4162.
[75] D. Cappus, M. Hassel, E. Neuhaus, M. Heber, F. Rohr and H.-J. Freund, *Surf. Sci.* **337** (1995), p. 268.
[76] G.T. Tyuliev and K.L. Kostov, *Phys. Rev. B* **60** (1999), p. 2900.
[77] C. Mocuta, A. Barbier, G. Renaud, M. Panabiere and P. Bayle-Guillemmaud, *J. Appl. Phys.* **95** (2004), p. 2151.